Single-cell polymer coating improves the desiccation tolerance of *Metarhizium brunneum* blastospores

Robin Dietsch[1][*] , Desiree Jakobs-Schönwandt[1,2] , Luisa Blöbaum[3] , Laila Bondzio[4],
Alexander Grünberger[5] and Anant Patel[1]

Abstract

Equipping cells with artificial shells or coats has been explored throughout the last decade, with goals such as immunomasking, in vivo tracing, and imparting tolerance to various biotic and abiotic stressors. One stressor, however, drying, has curiously been overlooked. In an industrial setting, the drying of cells is relevant when a satisfactory product shelf life must be achieved at a low cost. The drying of entomopathogenic organisms for biocontrol is a prime example of this. Here, the thin-walled blastospores of the entomopathogenic fungus *Metarhizium brunneum* are a great model organism for testing whether thin-cell surface polyelectrolyte layers may increase desiccation tolerance. In this study, we coated single *M. brunneum* blastospores with alternating layers of chitosan and alginate and assessed their effects on blastospore viability after drying. The desiccation tolerance improved with increasing layer numbers from 6.9% to a maximum of 27.5%. In addition, as the polymer chain length decreased, the desiccation tolerance further increased to 33.1%. Furthermore, we provided visual proof of the coating surrounding the blastospores via the use of fluorescent polymers and scanning electron microscopy. Finally, an investigation of differences in water absorption into coated and uncoated cells revealed that water absorbed faster into coated cells when alginate was on the surface of the structure but slower when the outermost layer was composed of chitosan. We conclude that, via polyelectrolyte multilayering on thin-walled blastospores, desiccation tolerance can be significantly increased, but a deeper understanding is necessary to extract the full potential from this technique.

Keywords Biocontrol, Desiccation tolerance, Formulation, Fungal blastospores, Polyelectrolyte multilayers, Single-cell
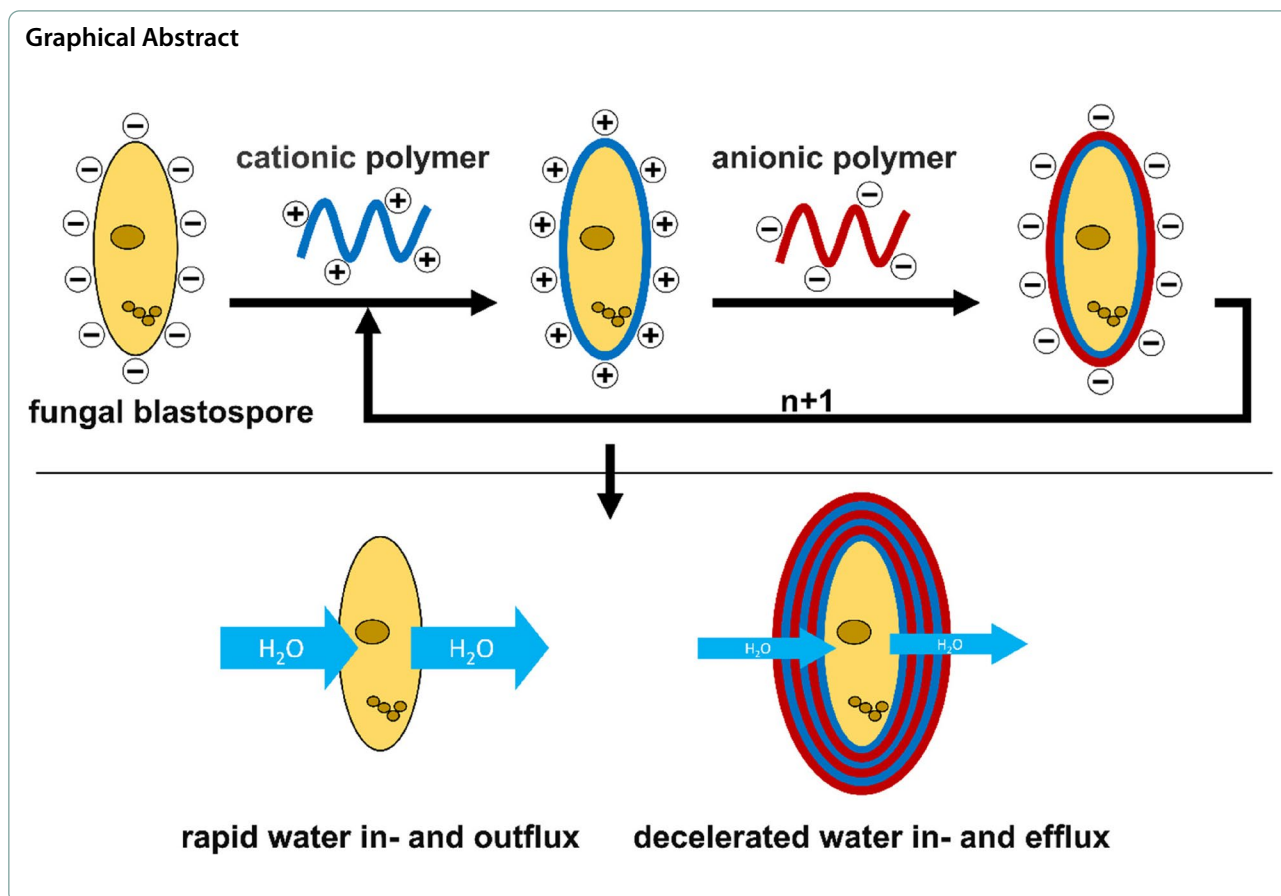
*Correspondence:
Robin Dietsch
robin.dietsch@outlook.com
Full list of author information is available at the end of the article

Graphical Abstract

Introduction

Desiccation, as a technique to prolong shelf-life, has significant industrial importance. The need for storage of biological materials, specifically cells, is encountered in many branches of biotechnology. Small-scale storage requirements, such as in-stock keeping, allow for liquid nitrogen, −80 ℃ freezing, or freeze-dried storage. These methods are well described, and protocols are readily available but are slow and/or expensive [6, 17, 65, 66], which limits the applicability of these techniques to certain industries. For other industries, with cheaper and larger scale requirements, dry storage is an appealing alternative.

Biological control is one such industry. Here, many products consist of living cells and need to achieve a certain shelf life at room temperature to be successfully commercialised [37, 47, 54]. Drying, however, drastically decreases the viability of most organisms [7, 11]. Such is the case with thin-walled, yeast-like blastospores, which many well-established biocontrol fungi form in submerged fermentation [33]. Their quick, highly advantageous fermentation process [22, 26] and high infectivity [1, 25, 38−40] have garnered

them great industrial interest. However, their low desiccation tolerance is a large obstacle to their profitable commercialisation [27]. Consequently, they greatly benefit from any improvements to their drying stability. For these reasons, we consider *Metarhizium brunneum* blastospores ideal candidates for novel formulations to increase desiccation tolerance.

While a dry cell is largely inert, severe stress is applied to the cells during de- and especially rehydration. These are time-critical processes, and their deceleration has been shown to lead to increases in bacterial viability [29, 43]. While deceleration of the drying process allows the cell to adapt to the changing environment metabolically through the accumulation of protectants [11], deceleration of the rehydration is largely beneficial on a physical basis. Rapid volume changes and the influx of water into a dry cell often rupture the dry and therefore inflexible cell membrane, leading to immediate cell death [11]. A physical barrier covering the cell surface of blastospores, through which water cannot freely move, slows the flux of water into and out of the cell during de- and rehydration and therefore decelerates these processes [67].

Dietsch *et al. Biotechnology for the Environment*   (2024) 1:13

Page 3 of 15

A possible solution is the concept of equipping living cells with an external shell structure by layer-by-layer (lbl) coating. Here, the electrostatic interaction between a material and the cell's own surface creates a material layer on the cell surface. Ideally, this layer deposition reverses the surface charge so that an oppositely charged material is adsorbed to the new surface (Fig. 1). With repeated application, multilayered single-cell complexes can be formed, typically in the range of 10–200 nm in thickness [10, 18, 48, 60, 64].

While most methods for producing coated cells are similar, the underlying goals vary. Most commonly, they lie either in biomedical applications [16, 42, 45, 51, 62, 63], or in the mimesis of bacterial sporulation to produce cells resistant to external stressors [13, 36, 46, 55, 68]. Whether polymer coats can improve the drying survival of cells, however, was not been investigated.

Owing to the demand for biocompatibility, biodegradability, and sufficient charge for lbl-coating, the choice of material is severely limited. In the food industry, biocompatible and biodegradable polymer layers are employed to act as moisture or air barriers for spoilable foods [4, 57]. Typically, consisting of hydrogel-forming biopolymers, their moisture barrier capabilities are rather limited [59, 71] but may be increased. The addition of a hydrophobic component reduces the water diffusion speed [2, 71], and blocking or shrinking voids within the hydrogel reduces the fast movement of free water [5, 14, 15, 53].

In the case of lbl-coatings, hydrophobic components would remain excluded from electrostatic interactions during the layering process and are therefore ill-suited. However, surface hydrophobisation may be possible by incorporating an amphiphile into the outermost layer. In some cases, chitosan has already displayed amphiphilic characteristics, unexpectedly increasing in hydrophobicity after drying [8]. In cellulose, this phenomenon is explained by the structural reorientation of the polymer chains, turning hydrophobic chain elements towards the air interface during drying [28]. The same mechanism is hypothesised to cause similar observations in chitosan films [20].

Schönhoff et al. [56] suggested that water diffusing out of polyelectrolyte multilayers creates voids or pores, which cannot be filled by the polymer due to steric hindrance of the polymer chains. Such pores allow for unhindered water flow during rehydration, which is undesirable because of the stress it imposes on the rehydrating cell. Research by Lin et al. [34] suggests that utilising shorter polymer chain lengths for polymer film production leads to increased surface coverage during the adsorption process of the polymer chains to the charged surface. As the production of polyelectrolyte multilayers is a succession of surface absorptions, the utilisation of shorter-chain polymers may decrease void formation through better coverage at the polymer-cell and subsequent polymer–polymer interfaces. Furthermore, steric hindrance to fill voids during desiccation may be decreased by shorter chain lengths, enabling the plugging of any voids [50].

At the surface level, cell encapsulation in a polymer matrix and single-cell coatings function in a similar way [21, 49, 61]. However, replacing a capsule that protects several cells in a bulk polymer mass with only a very thin and structured polymer shell that protects single cells, in theory disposes of several disadvantages of the bead or capsule approach but comes with certain trade-offs. As a byproduct of the single-cell approach, there is no waste of the active ingredient through agglomeration within the bulk polymer mass of a capsule. With a thin coating, every blastospore will have a minimum distance to the application target and an even distribution of all blastospores on the target can be achieved. In addition, through the order that is introduced into the polymer chains via electrostatic interactions, targeted surface modifications of the coated cell can be achieved [62]. Furthermore, shedding material obviously lowers the material cost. Other advantages include easy coapplication with other formulations and compatibility with many nozzle and hose types. This comes at the price of much less of a
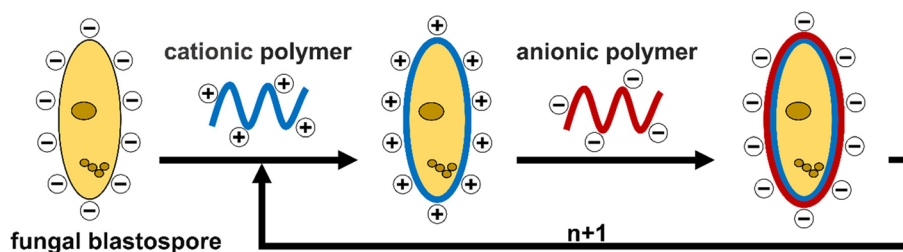

Fig. 1 Schematic of polyelectrolyte multilayer formation on a negatively charged cell surface. $n+1$ indicates the repeatability of the coating process, adding one polymer bilayer with every cycle

protective barrier between the blastospores and the environment. Where the coating may only have a protective function, a capsule is able to house nutrients and provide a growth-stimulating environment [21, 49, 61]. This function is lost by the coating, and part of this research aims to assess whether these advantages outweigh the disadvantages.

The aim of this study was to investigate the ability of biocompatible hydrogel-forming biopolymers encasing naturally thin-walled cells to improve their survival after dehydration, using *Metarhizium brunneum* CB15III blastospores as a model organism. By investigating water absorption into coated cells and the effect of the polymer chain length on viability, we take the first steps to understand the mode of action by which polyelectrolyte multilayers may improve the desiccation tolerance of single cells. The fermentation, drying, and rehydration techniques employed were specifically chosen to isolate the effects of the coating on blastospore drying survival by eliminating as many cross-effects as possible from established drying techniques, hyperosmotic stress conditioning during fermentation, and known formulation materials. We hypothesise that a cell surface polymer coat will improve the de- and rehydration characteristics in dependence on the polymer chain length and the outward-facing polymer, ultimately increasing blastospore viability after drying and rehydration. This approach lays the foundation for the potential of precisely targeted optimisations down the line.

Materials and methods
Aerial conidia production and harvest
Potato-dextrose agar (PDA, 39 g/L, Roth X931.2) plates inoculated with *M. brunneum* CB15III were incubated at room temperature until fully covered and sporulated, as indicated by the dark green color and the formation of a conidial powder on the plates. To harvest the aerial conidia, the plates were knocked several times and brushed with a sterilised brush to loosen any conidia still attached to the plate. The plates were then flushed repeatedly with 0.1%v/v Tween 80 (Carl Roth 9139.1) to suspend the conidia. Finally, the resulting conidial suspension was harvested from the plates by pipetting into 1.5-mL reaction tubes (Starlab TubeOne S16115-5500) and stored at 4 °C for up to 2 weeks. All steps were carried out under sterile conditions.

Blastospore production
Blastospores of *M. brunneum* were produced in baffled 250 mL shaker flasks filled with 75 mL fermentation medium (40 g/L AniPeptTM Animox; 55 g/L D-glucose monohydrate, Roth 6887.3; 70 g/L polyethylene glycol 200, Roth 2631.2; pH = 5.5). The flasks were inoculated by adding aerial conidia, which were subsequently suspended in 1 mL of 0.1%v/v Tween 80 to a final concentration of 1×10^5 conidia/mL. The cultivations were carried out for 96 h at 25 °C at 150 rpm (IKA KS 4000 ic control). This protocol was originally developed by Krell et al. [31] and its ingredients were screened to reduce pellet formation. After 72 h, the cultures were vacuum filtered through 12–15 μm paper filters (VWR 516–0350) to separate blastospores from the mycelial mass and immediately cooled to 4 °C. The resulting blastospore suspensions were washed thrice with 9 g/L sodium chloride solution (NaCl, Carl Roth P029.3) by centrifugation for 5 min at 2150×g and vortex resuspension (Vortex-Genie 2, Scientific Industries) in 50 mL centrifuge tubes (Greiner Bio-One, 227,270) filled to 40 mL. All blastospores were stored in 9 g/L NaCl solution at 4 °C for no longer than 24 h before experimental use. All steps were carried out under sterile conditions.

Polymer coating
To form the chitosan-alginate blastospore coating, 1×10^7 blastospores/mL suspended in 9 g/L NaCl solution were centrifuged for 5 min. The supernatant was discarded, and the blastospores were resuspended in 1 g/L chitosan solution under continuous agitation for 20 min at 4 °C. The blastospores were then washed once by centrifugation for 10 min and resuspended in NaCl solution. This was followed by two washing steps in the same solution with 5 min of centrifugation. All centrifugations were carried out at 2150×g and 4 °C. This procedure was then repeated with a 1 g/L alginate solution to create a bilayer. Subsequent bilayers were formed by alternation of the chitosan and alginate layer creation procedure. All alginate solutions were prepared by dissolving the respective alginate directly in ultrapure water (Elix Advantage 5, Merck). All chitosan solutions were prepared by first dissolving the respective chitosan powder at a concentration of 10 g/L in 1%v/v acetic acid (Roth 3738.3) under agitation for 24 h. Then, the resulting solution was diluted 1:10 with ultrapure water. All polymer solutions were vacuum filtered through a 12–15 μm filter to remove any macroparticles. The samples with zero bilayers were treated in the same manner but with a 9 g/L NaCl solution instead of a polymer solution. Any control samples were only washed three times in NaCl solution after harvest. Samples for de- and rehydration were always taken after three washing steps. All steps were carried out under sterile conditions. Three polymer solutions of varying chain lengths were produced from alginate and chitosan respectively. For these, relatively low, mediocre, and high molecular weights were chosen, labelled 'short', 'medium', and 'long', to indicate chain length. The polymer viscosity at a 2%w/v solution is universally given by the

manufacturers and chain lengths or molecular weights, if at all, only as calculations thereof. Therefore, the viscosity is given in Table 1 for comparability among the polymers.

Only polymers of 'medium' molecular weight were used in the viability determination, which was dependent on the number of polymer layers. For the viability determination, which was dependent on the polymer chain length, all the listed polymer solutions were used.

Dehydration and rehydration

For dehydration, 100 µL of treated or untreated blastospores suspended in a solution of 9 g/L NaCl at a concentration of 10^7 blastospores/mL were filled into previously detached and sterilised reaction tube lids. The lids were air dried in an enclosed container of 45 L with an air in- and outlet. An airflow of 10 L/min, 5% relative humidity, and 20 °C was applied for the entire duration. All samples were dried to a water activity of < 0.35 (LabMaster-aw, Novasina) or for a maximum of 48 h.

For rehydration, 1 mL reaction tubes without lids were filled with 1 mL of 9 g/L NaCl. The lids with dried blastospores were placed onto the filled reaction tubes, immediately inverted and vortexed for at least 1 min or until all the dried residue was removed from the lid. De- and rehydration were performed under sterile conditions at 20 °C.

Determination of viability/colony-forming units

This procedure always immediately followed rehydration. The blastospore suspension was diluted in 9 g/L NaCl so that approximately 200 viable blastospores in 10–100 µL of suspension could be transferred to a PDA plate. The proper dilution factors were determined from cell counts

prior to drying and estimates of viability taken from preliminary tests (data not shown). To determine the percentage of viable cells, a reference sample was taken from all samples immediately before drying. These were diluted and plated with 200 blastospores per plate. Generally, the colonies on all plates were counted after 72 h as they had a good size for counting at this point. After 96 h (24 h later) another plate check was performed to check for missed colonies during counting. Then survival was determined for all samples via the reference samples. All plates were inoculated and counted in triplicate in addition to the experimental replicates. The viability experiments were repeated once at a different time with the same results. The experimental data from repeated viability experiments is available in the Supplementary Materials 1 and 2.

Cell counting

All cell counting was conducted with a × 40 magnification objective via a transmitted-light microscope (Axiostar Plus, Zeiss) and a 'Neubauer Improved' cell counting chamber (Marienfeld Superior).

Fluorescence imaging

The images in Fig. 2 were taken with a × 100 objective via an inverted phase-contrast microscope (Nikon Eclipse Ti2, NIS Elements AR 5.20.01 Software, Nikon Instruments, Düsseldorf, Germany). The fluorescence filter details can be found in Table 2.

For bilayer visualisation, blastospores were coated with (A) one polymer bilayer consisting of fluorescein-labelled chitosan (FITC-chitosan) and rhodamine-labelled alginate (RH-alginate). The resulting coated blastospores

Table 1 List of polymers used

Polymer solution	Polymers and their viscosity at 2%w/v	Concentration [g/L]
Alginate solution 'short'	Na-Alginate, FMC Manucol DH, 40–90 cp	1
Alginate solution 'medium'	Na-Alginate FMC Manugel GMB, 110–270 cp	1
Alginate solution 'long'	Na-Alginate, Roth 9005–38-3, 350–550 cp,	1
Chitosan stock solution	Chitosan (s. columns below)	10
Chitosan solution 'short'	Chitosan, Sigma−Aldrich 448,869, 20–300 cp, 75–85% deactylated	1
Chitosan solution 'medium'	Chitosan, Sigma−Aldrich 448,877, 200–800 cp, 75–85% deactylated	1
Chitosan solution 'long'	Chitosan, Sigma−Aldrich 419,419, 800–2000 cp, 75–85% deactylated	1

Table 2 Fluorescence filter information

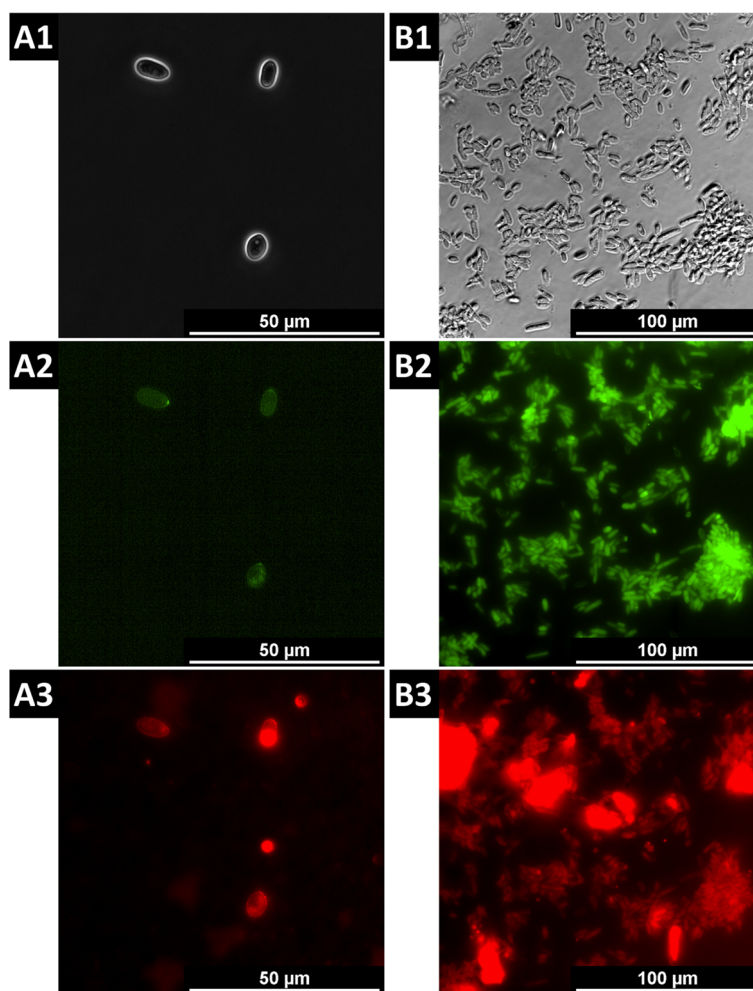| Filter	Excitation	Dichroic mirror	Emission	Product information
Green	472/30 nm	495 nm	520/35 nm	GFP-3035D Filter Cube, MXR00704, Nikon
Red	562/40 nm	593 nm	640/74 nm	mCherry-C Filter Cube, MXR00711, Nikon

Fig. 2 Blastospores coated with one bilayer of FITC-chitosan and RH-alginate (A1–A3) or three bilayers of chitosan and alginate, of which the outermost layer consisted of FITC-chitosan and RH-alginate (B1–B3). The images show the blastospores in phase contrast (A1, B1), green fluorescence (A2, B2) and red fluorescence (A3, B3) channels. × 1000 magnification

were analysed microscopically with the appropriate fluorescence channels. In the case of a successful initial bilayer formation in (A), the blastospores would fluoresce green and red in the appropriate channels. If only one polymer adhered to the spores, they would only fluoresce in that colour, and no further bilayer formation would theoretically occur.

To show evidence of bilayer formation beyond the initial bilayer, blastospores were coated with (B) two regular chitosan alginate bilayers and a third bilayer consisting of FITC-chitosan and RH-alginate. If no polymer adhered to the spores, again no fluorescence would occur. If only one polymer adhered to the spores, no fluorescence would occur either, as only the third bilayer contained fluorescently labelled polymers. The same is true if only one or two bilayers were able to adhere to the blastospores. Only if all three bilayers formed successfully green and

red fluorescence would be detectable in (B). The resulting coated blastospores were analysed microscopically with the appropriate fluorescence channels.

Scanning *electron* microscopy

The scanning electron microscopy images were produced with a FEI Helios NanoLab 600i dual beam-FIB at a voltage of 5 kV and a 0.17 nA beam current. For sample preparation, the coated and uncoated blastospores were dried in ultrapure water on silicon wafers and then sputtered with a ruthenium layer of approximately 5 nm under a vacuum.

Blastospore cell layer production and contact angle measurement

The blastospore cell layers were created by homogeneously depositing 5 mL of a 2×10^8 blastospores/mL

Dietsch *et al. Biotechnology for the Environment* (2024) 1:13

Page 7 of 15

suspension in ultrapure water onto a glass microscope slide (631–1550, VWR), leaving 5 mm of space to all edges. The suspension was allowed to air dry under sterile conditions, and the deposition was repeated once on top of the dried blastospores from the first deposition. Five slides with cell layers were created for every treatment.

For the contact angle measurements, 2 µL droplets of ultrapure water were deposited on the created blastospore layers, and droplet absorption and video recordings of droplet diffusion were taken via a dataphysics OCA 15Pro. The recorded contact angle changes were then analysed every 5 frames at 30 frames per second via SCA 20 software v.2. Every measurement was repeated five times, using a new slide with a new cell layer. The data was fitted by using the 'asymptotic fit' function in OriginPro 2022. All other fits produced less accurate models with lower R^2 (COD) values.

Statistical analysis

All statistical analyses were conducted via R. A generalised linear model was used to identify significant differences in the proportional data. Significant differences in the figures are indicated by letters. The values for p and n are denoted in the respective figure or table descriptions. The statistical differences in non-proportional data were determined by ANOVA and a post hoc Tukey test.

Results

Fluorescence-labelled polymers

Red and green fluorescent polymers were employed for bilayer visualisation. Blastospores coated with these polymers were observed microscopically in the appropriate fluorescence channels. The resulting images are shown in Fig. 2.

Figure 2(A1–A3) shows blastospores coated with a single bilayer of FITC-chitosan and RH-alginate. Figure 2(A1) shows the image in phase contrast, A2 shows the fluorescein channel, and A3 shows the rhodamine channel. The depicted blastospores fluoresce in the expected colors. Figure 2(B1–B3) shows blastospores coated with two bilayers of regular chitosan and alginate and a third bilayer of FITC-chitosan and RH-alginate. Figure 2(B1) shows the image in phase contrast, B2 in the fluorescein channel, and B3 in the rhodamine channel. The blastospores fluoresce green and red, respectively. Autofluorescence of untreated blastospores was not observed (Supplementary Materials 3).

This strongly indicates bilayer formation beyond an initial bilayer for the following reasons. The fluorescence in Fig. 2(A2 and A3) indicates the successful formation of an initial bilayer (Fig. 2(A1–A3)), as only a single bilayer was created in this case. The fluorescence in Fig. 2(B2 and B3) also indicates the successful formation of a bilayer but does not prove the formation of successive bilayers on its own. However, considering the successful formation of an initial bilayer (Fig. 2 A1–A3), it is a strong indicator of bilayer formation beyond the initial layer. It is unclear where the artefacts (bright spots) in images A3 and B3 originate, but as the majority of spores in the respective images are visible and fluorescent, we consider our arguments to be sound.

Scanning *electron* microscopy

To determine whether any polymer bilayers were directly observable, treated and untreated blastospores were dried and examined under a scanning electron microscope (SEM). The results are presented in Fig. 3.
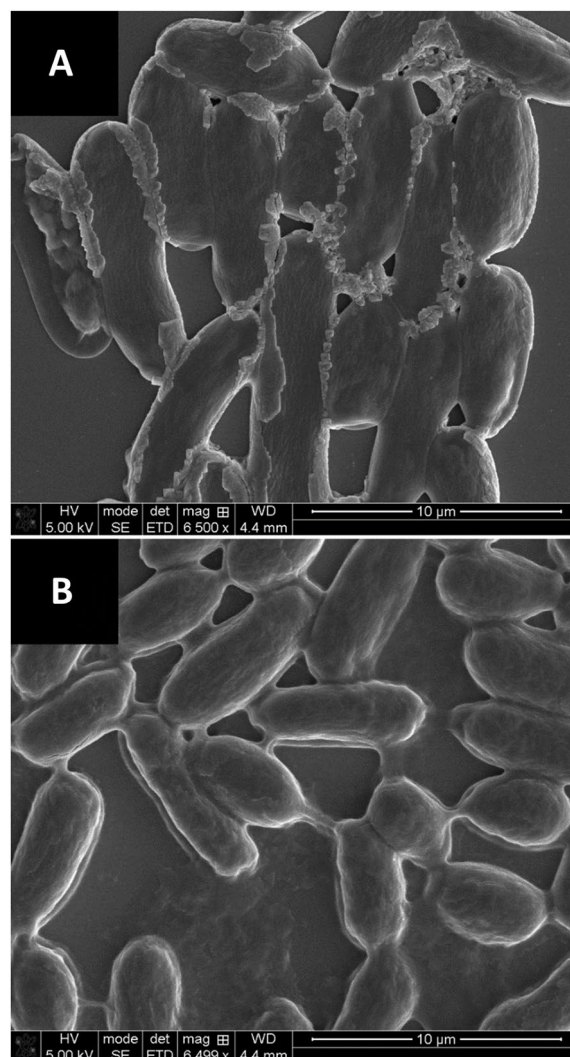

Fig. 3 Scanning electron microscopy images of uncoated (**A**) and coated (**B**) blastospores

Figure 3 shows uncoated (A) and coated blastospores (B) with three chitosan-alginate bilayers. In A, the blastospores appear to be predominantly naked, with the exception of a crystalline residue accumulated in some gaps between the spores. In contrast, the blastospores depicted in B appear to be coated with a thin material layer and even loosely stuck together by this substance. Furthermore, some of the substance also appears to have been deposited on the background material. There was no crystalline residue visible in B.

Contact angle measurement of blastospore cell films

To shed light on whether the coating reduces water influx into the cells during rehydration, a contact angle measurement over time was conducted on cell layers created from the coated and uncoated blastospores, as the water droplets are too large to deposit on single cells.

Because drops continuously diffuse into the cell layer, accurate determination of the surface energy was impossible. Nevertheless, drop adsorption kinetics could be recorded via the changing contact angles, as there is a linear relation between contact angle and absorbed drop volume on absorbent surfaces [30]. The initial contact angles after drop deposition were also considered when discussing the results. Figure 4 shows the contact angles over time.

All contact angle-time graphs decline asymptotically but follow different equation parameters. These and their significant differences are listed in Table 3. The mean contact angle of drops deposited on uncoated, alg-coated, and chi-coated blastospores decreased from 94.16° toward an asymptote of 19.23°, from 81.80° toward an asymptote of 12.17°, and from 81.84° toward an asymptote of 26.90°, respectively. The contact angle
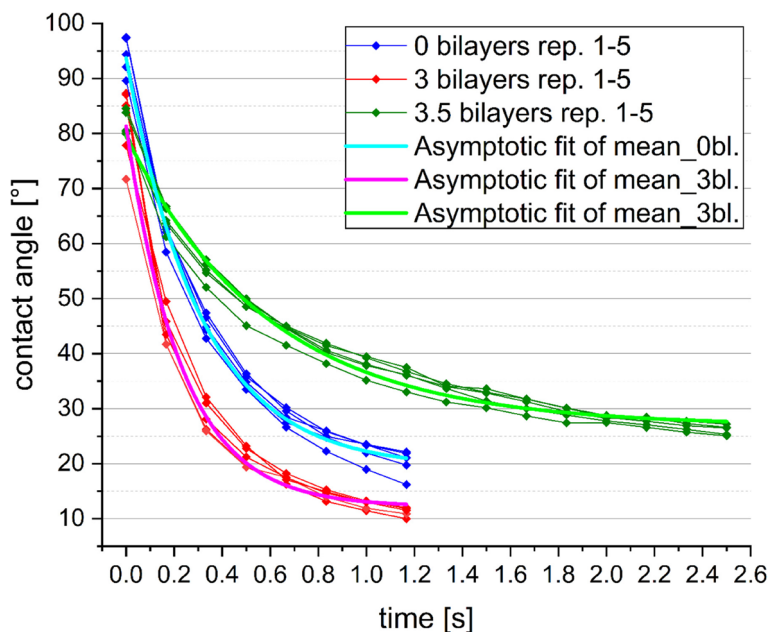

Fig. 4 Contact angles over time of uncoated blastospores (blue), blastospores coated with alginate on the outside (red) and blastospores coated with chitosan on the outside (green), and asymptotic fits of the means thereof. Blue: $y = 19.19 + 74.56 * 0.04^X$, R^2 (COD) = 0.99939. Red: $y = 12.03 + 69.41 * 0.02^X$, R^2 (COD) = 0.99822. Green: $y = 26.85 + 52.70 * 0.19^X$, R^2 (COD) = 0.99265. The use of a positively charged polymer (chitosan) must always be the first step of the bilayer (bl) creation process, therefore the number of applied layers cannot be equal among spores coated with different outer layers. Therefore, a 3-bilayer coating leads to alginate as the outermost layer (alg_coated), and a 3.5-bilayer coating leads to chitosan as the outermost layer (chi_coated). $n = 5$

Table 3 Equation factors of the asymptotic fits and their significant differences

Treatment	mean_a	sig_a	mean_b	sig_b	mean_c	sig_c
uncoated	19.19 ± 2.14	*a*	−74.56 ± 4.41	*a*	0.04 ± 0.01	*a*
alg_coated	12.03 ± 1.19	*b*	−69.41 ± 5.89	*a*	0.02 ± 0.01	*a*
chi_coated	26.85 ± 0.82	*c*	−52.70 ± 1.85	*b*	0.19 ± 0.03	*b*

Factor values derived from the exponential asymptotic equations used to approximate all absorption kinetics separately, not only the means depicted in Fig. 4. mean_a, mean_b, and mean_c refer to the factors a, b, and c from the employed exponential equation $y = a - b * c^X$. ± indicates the standard deviation. sig_a, sig_b, and sig_c show significant differences in lowercase letters and only compare differences within their respective columns (Anova + post hoc Tukey test, $n = 5$, $p < 0.05$)

changes of the uncoated and alg-coated blastospores were the most similar. There was no significant difference in slope (Table 3, mean_b, mean_c), but there was a significant difference in asymptote *y*-axis intercept elevation (Table 3, mean_a). Drops deposited on the surface of alg_coated blastospores presented 7.16° lower mean contact angles than did drops deposited on uncoated blastospores. Both graphs begin to closely approach their modelled asymptotes at approximately 1.2 s after drop deposition.

Notably, chi_coated blastospores display significantly greater overall contact angles, significantly greater final contact angles, and a significantly slower change than alg_coated and untreated blastospores do (Table 3). Conversely, the untreated blastospores presented significantly greater overall contact angles and significantly greater final contact angles than the alg-coated blastospores did, but no slower absorption occurred (Table 3).

Drops deposited on chi_coated blastospores behaved significantly differently from those deposited on alg_coated and uncoated blastospores in terms of the overall contact angle and contact angle change. The mean water contact angle of chi_coated blastospores was the highest overall, 7.67° greater than that of uncoated blastospores and 14.82° greater than that of alg_coated blastospores (Table 3, mean_a). Additionally, the decrease in the contact angle was less fast (Table 3, mean_b, mean_c), closely approaching its modelled asymptote of 26.85° within approximately 2.5 s.

Influence of polymer layers on desiccation tolerance

The aim of forming a cell surface polymer coating is to increase desiccation tolerance. In theory, every layer of material surrounding a cell, which acts as a steric barrier to water in- and outflux during de- and rehydration, should thus increase desiccation tolerance. Blastospores were equipped with zero to five polymer bilayers before drying and rehydration. Figure 5 shows the desiccation tolerance of blastospores in dependence on the number of cell surface polymer bilayers.

Figure 5 visualises the correlation between viability after de- and rehydration and an increase in the number of polymer bilayers on the blastospore cell surface. The viability increased from 6.9% (standard deviation (sd) = 4.2) to 14.2% (sd = 5.5), 23.3% (sd = 4.9), 24.8% (sd = 5.7) and 27.5% (sd = 4.5), with 0, 1, 3, 3.5 and 5 bilayers, respectively.

The increase caused by the addition of the first bilayer equates to a 106.1% increase in viability. The next increase by the addition of two further bilayers, however, only equates to an increase of 64.5%, or 32.3%, per bilayer. Finally, the addition of another two bilayers only increased the viability by 18.1%, or 9.0% per bilayer. The increase from three to five bilayers is not statistically significant and only adds to material and operational expenses, and blastospore loss during formulation, through unwanted blastospore aggregation with progressive layer formation was observed (Supplementary Materials 4). For this reason, the formation of three bilayers was chosen for further experiments as standard treatment.
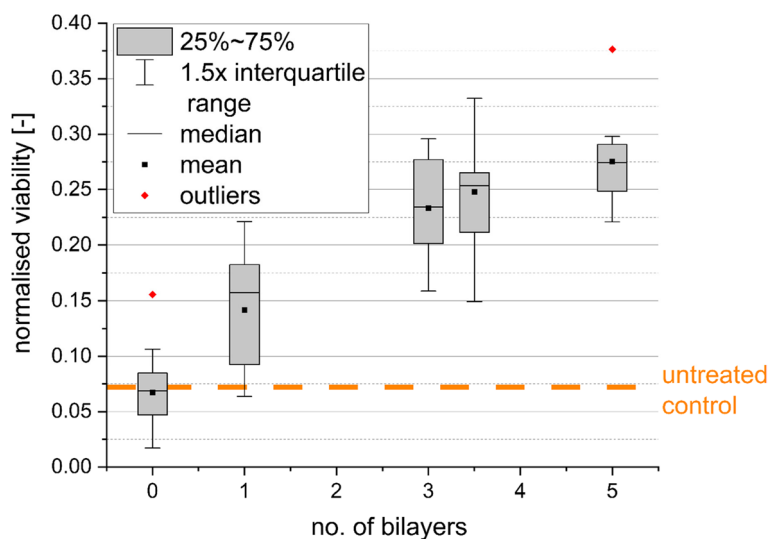

Fig. 5 Effect of the number of chitosan−alginate bilayers on blastospore survival after drying and rehydration. The error bars represent the standard deviation. Data for 3.5 bilayers was produced in a separate experiment. The control and data for 0 bilayers from both experiments were combined to show comparability. There is a significant increase in viability per layer (estimate of the logit model = 0.31527, std. error = 0.02965, $p < 0.001 = 1.19.10^{-14}$, $n = 9$). The data was normalised to the viability of the respective treatment before drying. Outliers are data points that lie outside of 1.5 × interquartile range and are shown in red. They are included in the calculation of the mean and median

Influence of the polymer chain length

The ability of polymer films to decelerate water flow is strongly dependent on the intermolecular makeup of the film. In repeated adsorption processes, as is the case with lbl-coating, decreasing the chain length of the polymers used may lead to less pore formation and consequently greater viability. To test this hypothesis, blastospores were equipped with three polymer bilayers of varying chain lengths before drying and rehydration. The resulting viabilities as a function of the polymer chain length after drying and rehydration are presented in Fig. 6.

Figure 6 reveals the significant influence of polymer chain length on desiccation tolerance, with increasing viabilities correlated with decreasing polymer chain length, as a decrease from 'long' to 'medium' resulted in significant a viability increase. This effect appears to be limited, however, as the viability increase from 'medium' to 'short' is not significant. The highest viability of 33.1% (sd = 10.3) was achieved when blastospores were coated with 'short' chain length chitosan and alginate. The 'medium' and 'long' chain lengths led to viabilities of 27.5% (sd = 10.2) and 13.4% (sd = 5.9), respectively. Uncoated blastospores reached a viability of 6.6% (sd = 2.8). When statistically analysing this data pooled with the data from the repeated experiment, all treatments are significantly different from one another (Supplementary Materials 6). In addition, the loss through spore aggregation during formulation was reduced when 'short' chitosan and alginate were used (Supplementary Materials 7).

Discussion

Before any potential benefit of the coating on desiccation tolerance can be determined, it is important to determine whether a successful coating was achieved. To confirm the successful coating process, two visual methods were chosen: coating with fluorescent polymers and scanning electron microscopy (SEM). Both visual confirmation methods strongly indicated successful coating formation, and Fig. 2 specifically shows successful bilayer formation beyond the initial layer.

The scanning electron microscopy images in Fig. 3 show uncoated blastospores (A) and coated blastospores (B) with three chitosan-alginate bilayers. In both images, the blastospores seem to have aggregated as a result of drying in a droplet on a flat surface. In A, the crystalline residue visible on the spores is likely a solute precipitate due to the increase in concentration from drying. It is unlikely, however, that the residue originates from the ultrapure water in which the blastospores are washed and suspended as part of SEM preparation. More likely, the blastospores released internal solutes to achieve osmotic balance when suspended in ultrapure water. Yeasts release glycerol in this situation, which could be the case here [3, 19, 58].

No other material is visible in Fig. 3A, and the blastospores appear largely uncovered. In contrast, the blastospores in Fig. 3B are clearly coated with a material layer that resembles other single-cell coats [48, 62, 68, 69]. We strongly suspect this to be the chitosan-alginate polymer
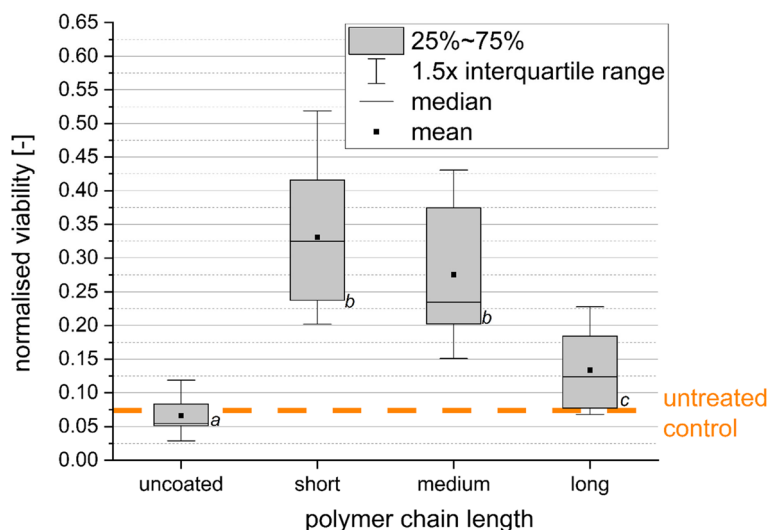

Fig. 6 Viabilities of blastospores with three chitosan-alginate bilayers in dependence of polymer chain length. Lowercase letters indicate statistically significant differences according to a general linear model (estimated differences of the logit model, $n = 10$, $p < 0.05$, standard errors and exact p values against all treatments are given in the Supplementary Materials 5). The data was normalised to the viability of the respective treatment before drying

Dietsch *et al. Biotechnology for the Environment* (2024) 1:13

Page 11 of 15

coating. Furthermore, there is no evidence of natural blastospore biofilm production that could produce similar visuals as in B. There is also no crystalline residue visible in B, perhaps suggesting that a polymer coat may hinder solutes from leaving the cells. This would be beneficial in cases of cell membrane rupture during rehydration and aid in upholding cellular gradients long enough for membrane repair [32]. Sakkos et al. [55] believe this to be the mode of action that stops enzyme leakage from dried and rehydrated *E. coli* to minimise the loss of biocatalyst activity.

Bilayer creation must not necessarily take place in full integer steps. For example, 3.5 bilayers consist of three full chitosan-alginate bilayers and an added single chitosan layer. This is relevant, as the outwards facing polymer may exhibit different and possibly beneficial properties, as previously discussed (' Introduction' section). Multiple sources suggest that increased hydrophobicity slows water diffusion [2, 71]. This phenomenon is explored in Fig. 4 via contact angle measurements. Contact angles greater than 90° generally indicate hydrophobic surfaces, while angles less than 90° indicate hydrophilic surfaces [70]. The greater initial contact angles induced by untreated blastospores suggest that both outwards-facing alginate and chitosan increased the hydrophilicity of blastospores in a dry state. Theoretically, these results are not unexpected for hydrogel-forming polymers. However, the literature suggests that chitosan polymer chains can rearrange themselves during desiccation to bury hydrophilic moieties within the bulk polymer and expose hydrophobic parts of the chain to the air interface, resulting in a surface with uncharacteristically high hydrophobicity [8, 20, 28]. Evidently, this is not the case for lbl-created chitosan-alginate films. In the referenced instances of chitosan or cellulose films displaying hydrophobic properties, the polymers were in homogenous form, in bulk, and not adsorbed to a surface via electrostatic interactions. This is not the case in lbl-film assembly. Perhaps, the very thin nature of the polymer layer and the interaction of presumably many charged groups within could restrict any free chain movement, or the degree of deacetylation of the used chitosan was too large, leaving too few hydrophobic moieties. No literature supports this hypothesis, however. The asymptotic decline of the contact angle to an apparent asymptote greater than zero is quite interesting on its own. With greater surface and presumably subsurface rewetting, absorption speed into the cell layer declines. It is conceivable that pores and other interstitial spaces are quickly filled and then water movement happens mainly by capillary action or diffusion through the hydrogel or extracellular matrix and cell wall, in the case of coated

and uncoated blastospores, respectively, simultaneously blocking bulk water influx from the outside.

Chitosan, as the outwards facing polymer, displayed more desirable properties than alginate in terms of hydrophobicity and absorption speed and therefore should lead to higher rates of survival after drying and rehydration. As shown in Fig. 5, however, this had no significant effect on viability. The increase in viability through the addition of 3.5 bilayers is in line with the expected increases provided by layer addition, independent of the specific outwards-facing polymer.

Figure 5 shows that the polymer coating is successful in increasing the desiccation tolerance to a certain degree. But, while viability improves with increasing layers, there are also diminishing returns relative to the first layer addition. Mondal and Mukherjee [44] reported that the reswelling of dry, thin, water-soluble polymer films is dependent on the polymer density, with denser films showing decreased diffusion when transitioning from a dry to a wet state. Moreover, Giermanska et al. [12] reported that the film density of thin polymer films is dependent on the film thickness. They provide an example of both increasing density with thickness and decreasing density with thickness and conclude that this behavior is polymer-dependent [12]. These principles may also apply to the present polyelectrolyte multilayers and thereby explain the observed behaviour. If the density of chitosan-alginate bilayers decreased with increasing coating thickness, then the rehydration speed, an important parameter for the survival of desiccation, would increase, and the viability would decrease. At the same time, however, the increase in bilayers leads to an increase in overall thickness and naturally leads to an overall improvement in desiccation tolerance via a longer diffusion path for water during de and rehydration. The combination of both effects could result in the observed decrease in viability per bilayer, as observed in Fig. 5. Unfortunately, there is no indication in the literature that alginate or chitosan behave in one of the ways described by Giermanska et al. [12].

The viability-chain length dependency shown in Fig. 6 suggests that a decrease in void formation could be hypothesised through the use of shorter polymer chain lengths, with the pooled data of both experiments pointing towards an even closer correlation. Of course, this hypothesis can neither be accepted nor rejected on the basis of viability alone. However, considering that the only difference in the experimental setup was the polymer chain length and that only de- and rehydration influence viability, the chain length must affect this process. The literature points towards decreased void formation [34, 50, 56]. Another factor, that may influence void

formation is the degree of chitosan deacetylation. In this study, all used chitosans were deacetylated to the same degree, but with an increase in charged groups, a denser, less porous chain packing might be achievable.

When the maximum achieved viability of 33.1% is compared to the viabilities reported in recent studies, specifically dedicated to enhancing blastospore survival rates for field application, there is a rather significant difference. Iwanicki et al., Mascarin et al. and Jackson et al., among others, reported viabilities of up to 80%, all while retaining pesticidal activity [22–24, 38, 41]. These are the results of fine-tuning many parameters that work together with additive effectiveness. Preconditioning and optimal media composition during fermentation, formulation additives, gentle drying techniques, naturally more desiccation-tolerant strains, and ideal rehydration conditions all contribute to the high achieved survival rates, far surpassing the viabilities achieved in this study [11]. This, however, was to be expected. To isolate the effect of polyelectrolyte multilayers on viability, no established techniques to increase blastospore desiccation tolerance were employed in this study. Additionally, the above-mentioned studies determined viability via observation of germ tube formation within a set amount of time [22–24, 38, 41]. This is not directly comparable with CFU analysis, as blastospores may form initial germ tubes, but not proliferate any further. These would not be detected in CFU analysis. On the other hand, some blastospores may ultimately form colonies but will have germinated much too slowly to be of use in a hypothetical application. Consequently, CFU analysis may more accurately reflect prolonged survival, but assaying germination is more application-oriented.

In terms of direct comparability, Sakkos et al. [55] present the most similar experimental conditions. In their study of the impact of a lbl-coating on the biocatalytic activity of *E. coli*, they also employed harsh drying conditions, which are not generally suitable for application, and focused on the singular effect of the coating. Their reported 6–sevenfold increase in biocatalytic activity compared with that of uncoated cells lies in the same regime as the fivefold increase reported here. Furthermore, the catalyst activity exhibited similar behaviour in relation to the number of bilayers applied, with large improvements in the initial layers, but plateauing between bilayers three and five. However, it is unclear whether the *E. coli* in this study actually remained viable, as Sakkos et al. [55] attributed the increase in catalytic activity to the ability of the coating to keep the enzymes encased in the structure regardless of cell life or death. It also remains unclear whether the plateauing of the catalyst activity is a result of increasing cell aggregation, as reported in this study. A comparison of the survival

rates of *M. brunneum* blastospores conventionally encapsulated in calcium alginate (Ca-alginate) beads can be found in Lorenz et al. [35]. The reported survival rates for multiple strains did not exceed 14.7%, indicating that the thickness of the hydrogel layer surrounding a cell is not representative of its drying survival.

Considering the results, we suggest polymer coat formulations to be used in conjunction with other formulation methods. Lbl-coats are situated in the sub-µm range of thickness and therefore do not interfere with other techniques such as conventional encapsulation or spray drying [9]. This allows formulations to prioritise other factors, such as UV protection or leaf adhesion or enables the use of harsher drying protocols.

Conclusion and outlook

Blastospores were coated with polyelectrolyte multilayers composed of chitosan and alginate. The addition of such a polymer coat, consisting of multiple layers on the blastospore cell surface, led to a significant increase in desiccation tolerance as a function of the number of produced bilayers and the chain length of the polymers. The successful layer formation was verified using fluorescent polymers and scanning electron microscopy. An analysis of the surface characteristics and water absorption into a dry layer of coated cells revealed that if chitosan was the air-interfacing polymer, the water contact angle was significantly greater, and water diffused significantly slower into the cells.

Compared with a study that similarly focused on investigating the isolated effect of a polyelectrolyte multilayer, the results clearly demonstrate the potential of biocompatible polyelectrolyte multilayers to protect against the loss of cell viability during de- and rehydration. It is obvious that employing this technique to improve desiccation tolerance is still in a proof-of-concept stage, with the underlying mechanisms not yet fully understood. This, however, implies that the application of this technique for this purpose is unoptimised and that further improvements are likely feasible. We have already demonstrated that by simply adjusting the polymer chain length, the viability could be improved, and the loss through aggregation decreased. Nevertheless, the highest viability of 33.1% is not yet enough to compete with application-oriented formulations or warrants the use of this technique in the fabrication of living cell products that are dried for storage. To extract the full potential of this technique, more light must be shed on the underlying mode(s) of action. This will allow targeted optimisation and improvement. Furthermore, this formulation can and should be applied in conjunction with other established techniques to improve desiccation tolerance. Currently, centrifugation steps complicate industrial scale-up, but

Dietsch *et al. Biotechnology for the Environment*   (2024) 1:13

Page 13 of 15

alternatives to centrifugation, such as cell separation via filtration or sedimentation, are conceivable. The polymer material usage is very low, and the downstream processing is concluded after the final wash of the cell suspension before dehydration. In conclusion, polyelectrolyte multilayers are promising prospects for flexible, desiccation-tolerant formulations of living cells.

Supplementary Information

The online version contains supplementary material available at https://doi.org/10.1186/s44314-024-00013-2.

> Supplementary Material 1: Supplementary Figure S1: Effect of number of polymer bilayers on viability after de- and rehydration. Figure 5 is an expanded repeated experiment of this data. There is a significant increase in viability per layer (estimate of the logit model = 0.643, std. error = 0.1015, $p < 0.001 = 0.000135$, $n = 4$, 0 bilayers $n = 3$). Supplementary Materials 2: Supplementary Figure S2: Effect polymer chain length treatment on viability after de- and rehydration. Figure 5 is a slightly expanded repeated experiment of this data. Outliers are data points that lie outside of 1.5 × interquartile range and are shown in red. They are included in the calculation of the mean and median. Lowercase letters indicate statistically significant differences according to a general linear model (estimated differences of the logit model, $n = 10$, $p < 0.05$, standard errors and exact p-values against all treatments are given in Supplementary Table S1 below). Supplementary Table S1: Statistical evaluation of Supplementary Fig. 2. Supplementary Materials 3: Supplementary Figure S3: Untreated Metarhizium brunneum blastospores in phase contrast, GFP, and MCherry fluorescence channels. Supplementary Materials 4: Supplementary Figure S4: Yield of viable M. brunneum blastospores post formulation, but before drying in dependence of the number of produced chitosan and alginate bilayers. Data related to the data shown in "Results—Influence of polymer layers on desiccation tolerance". Error bars show the standard deviation. There is a significant decrease in yield per layer (estimate of the logit model = —0.30694, std. error = 0.08951, $p < 0.001 = 0.0024$, $n = 6$). Supplementary Figure S5: Lightfield Microscopy Image of a blastospore aggregate. Supplementary Materials 5: Supplementary Table S2: Statistical evaluation of Fig. 6. Supplementary Materials 6: Supplementary Figure S6: Effect polymer chain length treatment on viability after de- and rehydration. This graph shows the pooled data of Fig. 5 and Supplementary Figure S2. Lowercase letters indicate statistically significant differences according to a general linear model (estimated differences of the logit model, $n = 20$ (pooled!), $p < 0.05$, standard errors and exact p-values against all treatments are given in Supplementary Table S3 below). Supplementary Table S3: Statistical evaluation of Supplementary Figure S5. Supplementary Materials 7: Supplementary Figure S7: Yield of viable M. brunneum blastospores post formulation, but before drying in dependence of the polymer chain length. Data related to the data shown in "Results—Polymer layers of different chainlengths". Error bars show the standard deviation. Lowercase letters indicate statistically significant differences according to a general linear model (estimated differences of the logit model, $n = 5$, $p < 0.05$, standard errors and exact p-values against all treatments are given in Supplementary Table S4 below). Supplementary Table S4: Statistical evaluation of Supplementary Figure S6.

Authors' contributions
RD conceived and wrote the main manuscript text. RD prepared all figures. RD conceived and conducted the experiments. LBl and LBo aided in data aquisition for Figures 2 and 3 respectively. RD, DSJ, and AP interpreted the results. RD, LBl, DSJ, AG and AP revised the manuscript. All Authors reviewed the manuscript.

Availability of data and materials
The raw and processed data required to reproduce these findings is available to download from https://doi.org/10.17632/46c36phyt4.1.

Declarations

Competing interests
The authors declare no competing interests.

Author details
[1]WG Fermentation and Formulation of Biologicals and Chemicals, Faculty of Engineering and Mathematics, Hochschule Bielefeld - University of Applied Sciences and Arts, Bielefeld, Germany. [2]Bioengineering and Sustainability, Westphalian University of Applied Sciences, Recklinghausen, Germany. [3]Multiscale Bioengineering, Technical Faculty, Bielefeld University, Bielefeld, Germany. [4]Thin Films and Physics of Nanostructures, Faculty of Physics, Bielefeld University, Bielefeld, Germany. [5]Institute of Process Engineering in Life Sciences: Microsystems in Bioprocess Engineering, Karlsruhe Institute of Technology, Karlsruhe, Germany.

References
1. Alkhaibari AM, Carolino AT, Yavasoglu SI, Maffeis T, Mattoso TC, et al. Metarhizium brunneum blastospore pathogenesis in Aedes aegypti larvae: attack on several fronts accelerates mortality. PLoS Pathog. 2016;12: e1005715. https://doi.org/10.1371/journal.ppat.1005715.
2. Balasubramanian R, Kim SS, Lee J. Novel synergistic transparent k-Carrageenan/Xanthan gum/Gellan gum hydrogel film: Mechanical, thermal and water barrier properties. Int J Biol Macromol. 2018;118:561–8. https://doi.org/10.1016/j.ijbiomac.2018.06.110.
3. Booth IR, Louis P. Managing hypoosmotic stress: aquaporins and medianosensitive channels in Escherichia coli. Curr Opin Microbiol. 1999;2(2):166–9. https://doi.org/10.1016/s1369-5274(99)80029-0.
4. Bourlieu C, Guillard V, Vallès-Pamiès B, Guilbert S, Gontard N. Edible moisture barriers: how to assess of their potential and limits in food products shelf-life extension? Crit Rev Food Sci Nutr. 2009;49(5):474–99. https://doi.org/10.1080/10408390802145724.
5. Cheng G-X, Liu J, Zhao R-Z, Yao K-D, Sun P-C, et al. Studies on dynamic behavior of water in crosslinked chitosan hydrogel. J Appl Polym Sci. 1998;67(6):983–8. https://doi.org/10.1002/(sici)1097-4628(19980207)67:6%3c983::Aid-app3%3e3.0.Co;2-i.
6. Coriell LL, Greene AE, Silver RK. Historical development of cell and tissue culture freezing. Cryobiology. 1964;1(1):72–9. https://doi.org/10.1016/0011-2240(64)90024-0.
7. Crowe JH, Hoekstra FA, Crowe LM. Anhydrobiosis. Annual Review of Physiology. 1992;54(1):579–99.
8. Cunha AG, Fernandes SCM, Freire CSR, Silvestre AJD, Neto CP, et al. What Is the Real Value of Chitosan's Surface Energy? Biomacromol. 2008;9(2):610–4. https://doi.org/10.1021/bm701199g.
9. Dai B, Wang L, Wang Y, Yu G, Huang X. Single-cell nanometric coating towards whole-cell-based biodevices and biosensors. ChemistrySelect. 2018;3(25):7208–21. https://doi.org/10.1002/slct.201800963.
10. Diaspro A, Silvano D, Krol S, Cavalleri O, Gliozzi A. Single living cell encapsulation in nano-organized polyelectrolyte shells. Langmuir. 2002;18(13):5047–50. https://doi.org/10.1021/la025646e.
11. Dietsch R, Jakobs-Schönwandt D, Grünberger A, Patel A. Desiccation-tolerant fungal blastospores: From production to application. Current Research in Biotechnology. 2021;3:323–39. https://doi.org/10.1016/j.crbiot.2021.11.005.
12. Giermanska J, Ben Jabrallah S, Delorme N, Vignaud G, Chapel J-P. Direct experimental evidences of the density variation of ultrathin polymer films with thickness. Polymer. 2021;228: 123934. https://doi.org/10.1016/j.polymer.2021.123934.

Dietsch *et al. Biotechnology for the Environment*   (2024) 1:13

Page 14 of 15

13. Gould GW. BACTERIA | bacterial endospores. Encyclopedia of Food Microbiology. 1999;168–173. https://doi.org/10.1006/rwfm.1999.0135.

14. Gun'ko VM, Savina IN, Mikhalovsky SV. Properties of water bound in hydrogels. Gels. 2017;3(4). https://doi.org/10.3390/gels3040037.

15. Guo W, Chen J, Sun S, Zhou Q. Investigation of water diffusion in hydrogel pore-filled membrane via 2D correlation time-dependent ATR-FTIR spectroscopy. J Mol Struct. 2018;1171:600–4. https://doi.org/10.1016/j.molstruc.2018.06.048.

16. Hashemi-Najafabadi S, Vasheghani-Farahani E, Shojaosadati SA, Rasaee MJ, Armstrong JK, et al. A method to optimize PEG-coating of red blood cells. Bioconjugate Chem. 2006;17(5):1288–93. https://doi.org/10.1021/bc060057w.

17. Hess JR. Red cell storage. J Proteomics. 2010;73(3):368–73. https://doi.org/10.1016/j.jprot.2009.11.005.

18. Hillberg AL, Tabrizian M. Biorecognition through layer-by-layer polyelectrolyte assembly: in-situ hybridization on living cells. Biomacromol. 2006;7(10):2742–50. https://doi.org/10.1021/bm060266j.

19. Hohmann S. Osmotic stress signaling and osmoadaptation in yeasts. Microbiol Mol Biol Rev. 2002;66(2):300. https://doi.org/10.1128/mmbr.66.2.300-372.2002.

20. Hubbe MA. Why, after all, are chitosan films hydrophobic? BioResources. 2019;14(4):7630–1.

21. Humbert P, Przyklenk M, Vemmer M, Patel AV. Calcium gluconate as cross-linker improves survival and shelf life of encapsulated and dried Metarhizium brunneum and Saccharomyces cerevisiae for the application as biological control agents. J Microencapsul. 2017;1–31. https://doi.org/10.1080/02652048.2017.1282550.

22. Iwanicki NSA, Ferreira BDO, Mascarin GM, Delalibera Junior I. Modified Adamek's medium renders high yields of Metarhizium robertsii blastospores that are desiccation tolerant and infective to cattle-tick larvae. Fungal Biol-Uk. 2018;122(9):883–90. https://doi.org/10.1016/j.funbio.2018.05.004.

23. Iwanicki NSA, Mascarin GM, Moreno SG, Eilenberg J, Delalibera I. Development of novel spray-dried and air-dried formulations of Metarhizium robertsii blastospores and their virulence against Dalbulus maidis. Appl Microbiol Biotechnol. 2021;105(20):7913–33. https://doi.org/10.1007/s00253-021-11576-5.

24. Jackson MA, Mascarin GM, 2016. Stable fungal blastospores and methods for their production, stabilization and use, in: Office, C.I.P. (Ed.) A01N 63/02 (2006.01) ed. EMBRAPA, US Department of Agriculture Canada.

25. Jackson MA, Mcguire MR, Lacey LA, Wraight SP. Liquid culture production of desiccation tolerant blastospores of the bioinsecticidal fungus Paecilomyces fumosoroseus. Mycol Res. 1997;101:35–41. https://doi.org/10.1017/S0953756296002067.

26. Jaronski S. Mass production of entomopathogenic fungi—state of the art. In: Morales-Ramos JA, Guadalupe Rojas M, Shapiro-Ilan DI, editors. Mass Production of Beneficial Organisms: Invertebrates and Entomopathogens. San Diego: Academic Press; 2013. p. 357–413.

27. Jaronski ST, Mascarin GM. Mass production of fungal entomopathogens. In: Lacey LA, editor. Microbial control of insect and mite pests: from theory to practice. London: Elsevier Science; 2016. p. 141–56.

28. Khayet M, Essalhi M. Effects of surface modifying macromolecules on the structural characteristics of different structured and nanofibrous membranes. 2015.

29. Kosanke JW, Osburn RM, Shuppe GI, Smith RS. Slow rehydration improves the recovery of dried bacterial populations. Can J Microbiol. 1992;520–525. https://doi.org/10.1139/m92-086.

30. Krainer S, Hirn U. Contact angle measurement on porous substrates: Effect of liquid absorption and drop size. Colloids Surf, A. 2021;619: 126503. https://doi.org/10.1016/j.colsurfa.2021.126503.

31. Krell V, Jakobs-Schoenwandt D, Vidal S, Patel AV. Encapsulation of Metarhizium brunneum enhances endophytism in tomato plants. Biol Control. 2018;116:62–73. https://doi.org/10.1016/j.biocontrol.2017.05.004.

32. Lebre PH, De Maayer P, Cowan DA. Xerotolerant bacteria: surviving through a dry spell. Nat Rev Microbiol. 2017;15(5):285–96. https://doi.org/10.1038/nrmicro.2017.16.

33. Leland JE, Mullins DE, Vaughan LJ, Warren HL. Effects of media composition on submerged culture spores of the entomopathogenic fungus, Metarhizium anisopliae var. acridum Part 2: Effects of media osmolality

on cell wall characteristics, carbohydrate concentrations, drying stability, and pathogenicity. Biocontrol Sci Techn. 2005;15(4):393–409.

34. Lin EY, Frischknecht AL, Winey KI, Riggleman RA. Effect of surface properties and polymer chain length on polymer adsorption in solution. J Chem Phys. 2021;155(3): 034701. https://doi.org/10.1063/5.0052121.

35. Lorenz S-C, Humbert P, Patel AV. Chitin increases drying survival of encapsulated Metarhizium pemphigi blastospores for Ixodes ricinus control. Ticks Tick-borne Dis. 2020;11(6): 101537. https://doi.org/10.1016/j.ttbdis.2020.101537.

36. Magrassi R, Ramoino P, Bianchini P, Diaspro A. Protection capabilities of nanostructured shells toward cell encapsulation: a saccharomyces/paramecium model. Microsc Res Tech. 2010;73(10):931–6. https://doi.org/10.1002/jemt.20844.

37. Malusá E, Sas-Paszt L, Ciesielska J. Technologies for beneficial microorganisms inocula used as biofertilizers. Sci World J. 2012;2012. https://doi.org/10.1100/2012/491206.

38. Mascarin GM, Jackson MA, Behle RW, Kobori NN, Delalibera I. Improved shelf life of dried Beauveria bassiana blastospores using convective drying and active packaging processes. Appl Microbiol Biot. 2016;100(19):8359–70. https://doi.org/10.1007/s00253-016-7597-2.

39. Mascarin GM, Jackson MA, Kobori NN, Behle RW, Delalibera Júnior Í. Liquid culture fermentation for rapid production of desiccation tolerant blastospores of Beauveria bassiana and Isaria fumosorosea strains. J Invertebr Pathol. 2015;127:11–20. https://doi.org/10.1016/j.jip.2014.12.001.

40. Mascarin GM, Jackson MA, Kobori NN, Behle RW, Dunlap CA, et al. Glucose concentration alters dissolved oxygen levels in liquid cultures of Beauveria bassiana and affects formation and bioefficacy of blastospores. Appl Microbiol Biot. 2015b;99(16):6653–65.

41. Mascarin GM, Kobori NN, Jackson MA, Dunlap CA, Delalibera Í. Nitrogen sources affect productivity, desiccation tolerance and storage stability of Beauveria bassiana blastospores. J Appl Microbiol. 2018;124(3):810–20. https://doi.org/10.1111/jam.13694.

42. Michalet X, Pinaud FF, Bentolila LA, Tsay JM, Doose S, et al. Quantum dots for live cells, in vivo imaging, and diagnostics. Science. 2005.

43. Mille Y, Beney L, Gervais P. Magnitude and kinetics of rehydration influence the viability of dehydrated E. coli K-12. Biotechnol Bioeng. 2003;83(5):578–82. https://doi.org/10.1002/bit.10706.

44. Mondal MH, Mukherjee M. Study of density-dependent swelling of ultrathin water soluble polymer films. J Polym Res. 2014;21(2):1–6. https://doi.org/10.1007/s10965-013-0343-x.

45. Nacharaju P, Boctor FN, Manjula BN, Acharya SA. Surface decoration of red blood cells with maleimidophenyl-polyethylene glycol facilitated by thiolation with iminothiolane: an approach to mask A, B, and D antigens to generate universal red blood cells. Transfusion. 2005;45(3):374–83. https://doi.org/10.1111/j.1537-2995.2005.04290.x.

46. Park JH, Kim K, Lee J, Choi JY, Hong D, et al. A cytoprotective and degradable metal–polyphenol nanoshell for single-cell encapsulation. Angew Chem Int Ed. 2014;53(46):12420–5. https://doi.org/10.1002/anie.201405905.

47. Parnell JJ, Berka R, Young HA, Sturino JM, Kang Y, et al. From the lab to the farm: an industrial perspective of plant beneficial microorganisms. Front Plant Sci. 2016;7. https://doi.org/10.3389/fpls.2016.01110.

48. Peil S, Beckers SJ, Fischer J, Wurm FR. Biodegradable, lignin-based encapsulation enables delivery of Trichoderma reesei with programmed enzymatic release against grapevine trunk diseases. Materials Today Bio. 2020;7: 100061. https://doi.org/10.1016/j.mtbio.2020.100061.

49. Przyklenk M, Vemmer M, Hanitzsch M, Patel A. A bioencapsulation and drying method increases shelf life and efficacy of *Metarhizium brunneum* conidia. J Microencapsul. 2017;34(5):498–512.

50. Reineccius GA, Yan C. Factors controlling the deterioration of spray dried flavourings and unsaturated lipids. Flavour Fragr J. 2016;31(1):5–21. https://doi.org/10.1002/ffj.3270.

51. Rogers WJ, Meyer CH, Kramer CM. Technology Insight: in vivo cell tracking by use of MRI - Nature Reviews Cardiology. Nat Rev Cardiol. 2006;3:554–62. https://doi.org/10.1038/ncpcardio0659.

52. Rossi NaA R, Constantinescu I, Kainthan RK, Brooks DE, Scott MD, et al. Red blood cell membrane grafting of multi-functional hyperbranched polyglycerols. Biomaterials. 2010;31(14):4167–78. https://doi.org/10.1016/j.biomaterials.2010.01.137.

53. Rostovtseva TK, Bashford CL, Alder GM, Hill GN, Mcgiffert C, et al. Diffusion through narrow pores: movement of ions, water and nonelectrolytes

Dietsch *et al. Biotechnology for the Environment*   *(2024) 1:13*

Page 15 of 15

through track-etched PETP membranes. J Membr Biol. 1996;151(1):29–43. https://doi.org/10.1007/s002329900055.

54. Sahu PK, Gupta A, Singh M, Mehrotra P, Brahmaprakash GP. Bioformulation and fluid bed drying: a new approach towards an improved biofertilizer formulation. SpringerLink. 2018;47–62. https://doi.org/10.1007/978-981-10-6934-5_3.

55. Sakkos JK, Wackett LP, Aksan A. Enhancement of biocatalyst activity and protection against stressors using a microbial exoskeleton - Scientific Reports. Sci Rep. 2019;9(3158):1–12. https://doi.org/10.1038/s41598-019-40113-8.

56. Schönhoff M, Ball V, Bausch AR, Dejugnat C, Delorme N, et al. Hydration and internal properties of polyelectrolyte multilayers. Colloids Surf, A. 2007;303(1–2):14–29.

57. Singha K, Rohit K (2023) Hydrogel-Based Food Packaging Films, Natural materials for food packaging application. Wiley-VCH GmbH, Weinheim, Germany, pp. 89–103.

58. Tamás MJ, Luyten K, Sutherland FCW, Hernandez A, Albertyn J, et al. Fps1p controls the accumulation and release of the compatible solute glycerol in yeast osmoregulation. Mol Microbiol. 1999;31(4):1087–104. https://doi.org/10.1046/j.1365-2958.1999.01248.x.

59. Tapia MS, Rojas-Graü MA, Rodríguez FJ, Ramírez J, Carmona A, et al. Alginate- and Gellan-based edible films for probiotic coatings on fresh-cut fruits. J Food Sci. 2007;72(4):E190–6. https://doi.org/10.1111/j.1750-3841.2007.00318.x.

60. Van Der Meeren L, Verduijn J, Li J, Verwee E, Krysko DV, et al. Encapsulation of cells in gold nanoparticle functionalized hybrid layer-by-layer (LbL) hybrid shells – remote effect of laser light. Applied Surface Science Advances. 2021;5: 100111. https://doi.org/10.1016/j.apsadv.2021.100111.

61. Vemmer M, Patel AV. Review of encapsulation methods suitable for microbial biological control agents. Biol Control. 2013;67(3):380–9. https://doi.org/10.1016/j.biocontrol.2013.09.003.

62. Wang B, Liu P, Jiang W, Pan H, Xu X, et al. Yeast cells with an artificial mineral shell: protection and modification of living cells by biomimetic mineralization. Angew Chem Int Ed. 2008;47(19):3560–4. https://doi.org/10.1002/anie.200704718.

63. Wang D, Toyofuku WM, Scott MD. The potential utility of methoxypoly(ethylene glycol)-mediated prevention of rhesus blood group antigen RhD recognition in transfusion medicine. Biomaterials. 2012;33(10):3002–12. https://doi.org/10.1016/j.biomaterials.2011.12.041.

64. Wang L, Li Y, Yang X-Y, Zhang B-B, Ninane N, et al. Single-cell yolk-shell nanoencapsulation for long-term viability with size-dependent permeability and molecular recognition. Natl Sci Rev. 2021;8(4). https://doi.org/10.1093/nsr/nwaa097.

65. Wilkinson T, Wetten A, Prychid C, Fay MF. Suitability of cryopreservation for the long-term storage of rare and endangered plant species: a case history for cosmos atrosanguineus. Ann Bot. 2003;91(1):65–74. https://doi.org/10.1093/aob/mcg009.

66. Wolkers WF, Tablin F, Crowe JH. From anhydrobiosis to freeze-drying of eukaryotic cells. Comp Biochem Physiol A: Mol Integr Physiol. 2002;131(3):535–43. https://doi.org/10.1016/s1095-6433(01)00505-0.

67. Yang C, Xing X, Li Z, Zhang S. A comprehensive review on water diffusion in polymers focusing on the polymer–metal interface combination. Polymers. 2020;12(1):138. https://doi.org/10.3390/polym12010138.

68. Yang SH, Kang SM, Lee K-B, Chung TD, Lee H, et al. Mussel-inspired encapsulation and functionalization of individual yeast cells. J Am Chem Soc. 2011;133(9):2795–7. https://doi.org/10.1021/ja1100189.

69. Yang SH, Lee K-B, Kong B, Kim J-H, Kim H-S, et al. Biomimetic encapsulation of individual cells with silica. Angew Chem Int Ed. 2009;48(48):9160–3. https://doi.org/10.1002/anie.200903010.

70. Yuan Y, Lee TR. Contact angle and wetting properties. In: Bracco G, Holst B, editors. Surface science techniques. Heidelberg: Springer; 2013. p. 3–34.

71. Zukas BG, Gupta NR. Improved water barrier properties of calcium alginate capsules modified by silicone oil. Gels. 2016;2(2):14. https://doi.org/10.3390/gels2020014.

Publisher's Note

Springer Nature remains neutral with regard to jurisdictional claims in published maps and institutional affiliations.